Int. J. Electrochem. Sci., 15 **(2020)** 8498 – 8505, doi: 10.20964/2020.09.46

International Journal of
ELECTROCHEMICAL
SCIENCE
www.electrochemsci.org

Short Communication

Aluminum Electrodeposition using $AlCl_3$/urea Ionic Liquid

Min Li[1,2,3,*] , *Ying Li*[1,2,*]

[1] School of Metallurgy, Northeastern University, Shenyang 110819, China
[2] Liaoning Key Laboratory for Metallurgical Sensor and Technology, Northeastern University, Shenyang 110819, China
[3] Key Laboratory for Ecological Metallurgy of Multimetallic Mineral, Ministry of Education, Shenyang 110819, China
[*]E-mail: lim@smm.neu.edu.cn; gaoanlimin@163.com

Received: 3 May 2020 / *Accepted:* 27 June 2020 / *Published:* 10 August 2020

Aluminum electrodeposition using $AlCl_3$/urea ionic liquid was studied at 333 K. Raman spectra and cyclic voltammetry results show that aluminum can be electrodeposited from such ionic liquids having $AlCl_3$:urea molar ratios above 1.2. Moreover, the molar ratio of the ionic liquid has an obvious effect on the aluminum species and electrochemical behavior of Al(III). Potentiostatic electrolysis experiments were conducted on the ionic liquid to prepare metallic coatings, and the obtained coatings were characterized using scanning electron microscopy energy dispersive spectroscopy (SEM–EDS) and X-ray powder diffraction (XRD) techniques. SEM analysis shows that needle-like and cauliflower-like coatings, characterized to be metallic aluminum by the EDS and XRD, were obtained at 313 and 333 K, respectively. This method can provide a new and inexpensive candidate medium for aluminum recycling at room temperature.

Keywords: aluminum; electrodeposition; ionic liquid; Raman spectra; cyclic voltammetry

1. INTRODUCTION

Aluminum and its alloys have attracted considerable attention because of their excellenct physical and chemical properties, and have been widely used in various fields [1–4], particularly in energy storage technology owing to the development of the rechargeable aluminum-ion battery [5–13]. The Hall–Heroult process is the well-known traditional industrial method for fabricating aluminum; however, it should be conducted at temperatures above 1173 K. Therefore, ionic liquids that can be used for metal electrodeposition at room temperature have received considerable attention.

The electrochemical reduction behavior of Al(III) has been widely reported in chloroaluminate electrolytes. Brisard et al. [14] reported the deposition and surface morphology of aluminum on

tungsten and aluminum substrates in $AlCl_3$–EMImCl (1-ethyl-3-methylimidazolium chloride) ionic liquid. Their chronoamperogram analysis indicated that the electroreduction of Al(III) on a tungsten substrate followed an instantaneous nucleation model, while the reduction of Al(III) at aluminum electrode was due to kinetic limitations. Scanning electron microscopy (SEM) analysis revealed that the deposits obtained on both tungsten and aluminum substrates were dense and adherent. Li et al. [15] investigated the reduction of Al(III) from $AlCl_3$–EMImCl ionic liquid in the presence and absence of saturated $LaCl_3$ using different methods. They studied the surface morphology and grain size of electrodeposit at various parameters and concluded that electrodeposits obtained using a pulse-current method exhibited a flatter and brighter surface than those obtained using a direct-current method, and the electrodeposit morphology was significantly affected by temperature and pulse-current frequency. The grain size of electrodeposits increased with increasing temperature. A small and sphere-like electrodeposit structure was exhibited at 298 K, whereas a feather-like electrodeposit structure was exhibited at 363 K. Additionally, they found that the addition of $LaCl_3$ to the ionic liquid effectively lowered electrodeposit porosity while enhancing compactness. Neubert et al. [16,17] researched the electrochemical and corrosion behavior of the obtained micro- and nano-crystalline aluminum in $AlCl_3$–EMImCl ionic liquid. Cyclic voltammetry analysis indicated that the reduction of aluminum was a quasi-reversible reaction controlled by charge-transfer kinetics and diffusion of electroactive species. Dense and adherent nano-crystalline aluminum deposits were obtained at more negative potentials owing to the growth inhibition of aluminum crystallites by organic species. X-ray powder diffraction (XRD) analysis revealed that nano-crystalline aluminum electrodeposits showed an average crystallite size of 177 nm at −0.6 V, but an average crystallite size of 28 nm at −0.7 V. Furthermore, the nano-crystalline aluminum was more corrosion-resistance than the micro-crystalline aluminum. Endres et al. [18] studied the electrodeposition of aluminum on mild steel in $AlCl_3$–EMImCl ionic liquid. The results showed that the pretreatment of the substrates played a key role in coating adhesion. They found that aluminum coatings with good adherence capable of resisting even mechanical scratching were obtained using in situ electrochemical etching of the substrate by anodic polarization prior to electrodeposition. Aluminum alloys obtained from ionic liquids have also been comprehensively reported in the literature [19–23]. Other researchers have studied the electrochemical behavior of aluminum not only in the aforementioned chloroaluminate ionic liquids but also in some newly developed ionic liquids [24–30].

In this study, the electrochemical reduction of Al(III) in $AlCl_3$/urea ionic liquid was investigated. SEM, energy dispersive spectroscopy (EDS), and XRD techniques were used to characterize the deposits.

2. EXPERIMENTAL

EMImCl (Aladdin, 98%) and anhydrous $AlCl_3$ (Aladdin, 99%) were used directly without any purification. Urea (Sinopharm Chemical Reagent Co., Ltd, China, ≥98.5%) was pretreated for one day at 393 K under vacuum. $AlCl_3$/urea ionic liquids were synthesized by slowly mixing $AlCl_3$ and urea in a sealed vessel at room temperature under a high-purity argon atmosphere in a glove box (MBRAUN MB 200B, Germany), where both the water and oxygen contents were maintained below 0.1 ppm. The

solids reacted immediately without external heating and were left to cool gradually to room temperature. Homogeneous and transparent $AlCl_3$/urea ionic liquids were formed at $AlCl_3$/urea molar ratios of 1.2, 1.3, and 1.5.

A Raman spectrometer (Horiba Jobin Yvon LabRAM XploRA, France) attached with a laser was used to record the Raman spectra. A KIMMON KOHA kR1801C He-Cd laser (20 mW, 325 nm) was used to generate the exciting laser and an Olympus micro objective (10 × 0.25) was used for observing the samples that were sealed in the glove box. An AUTOLAB (Metrohm PGSTAT 30, Switzerland) electrochemical workstation was used to perform the cyclic voltammetry (CV) measurements using a three-electrode cell under an argon atmosphere. A tungsten wire (Alfa Aesar, ≥99.95%, 1 mm diameter, 0.157 cm^2 working area), a high-purity aluminum wire (Alfa Aesar, ≥99.99%), and a platinum wire (Alfa Aesar, ≥99.99%) were used as the working electrode, reference electrode, and quasi-reference electrode, respectively. The lower end of the working electrode was thoroughly polished with sandpaper, cleaned in ethanol using an ultrasonic cleaner, rinsed with distilled water, and finally dried before measurements. The immersion depth (0.5 cm) of the working electrode in the ionic liquid was kept the same for each experiment.

The potentiostatic electrolysis experiments were performed on a copper plate (Alfa Aesar, 99.99%, 0.25 cm^2) under an argon atmosphere for 2 h. The aluminum electrodeposits were cleaned with anhydrous ethanol to remove residual ionic liquids. A high-resolution scanning electron microscope (SEM, Shimadzu SSX-550, Japan) attached with energy dispersive spectroscope (EDS) working at 15 kV was utilized to study the surface morphologies and compositions of the aluminum electrodeposits. A X-ray diffraction (XRD, PANalytical MPDDY 2094, Netherlands) using Cu Kα line working at 40 kV and 40 mA was used to determine the phases and structures of the samples.

3. RESULTS AND DISCUSSION

3.1. Raman spectroscopy

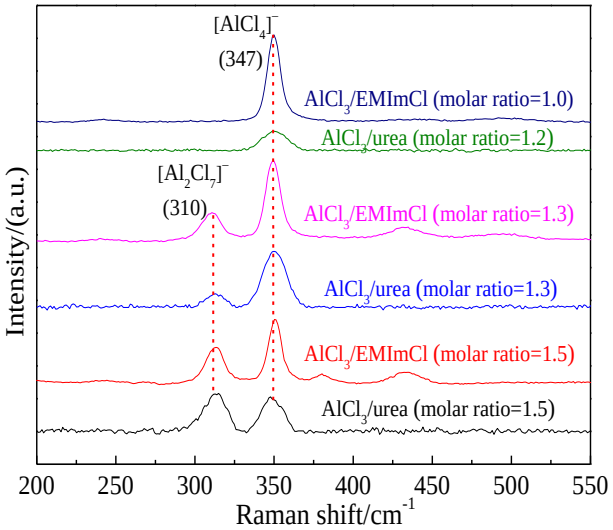

Figure 1. Raman spectra of $AlCl_3$/urea ionic liquid with $AlCl_3$:urea molar ratios of 1.2, 1.3, and 1.5 and $AlCl_3$/EMImCl ionic liquid with $AlCl_3$:EMImCl molar ratios of 1.0, 1.3, and 1.5 recorded at 333 K.

Fig. 1 presents the Raman spectra of $AlCl_3$/urea ionic liquid with $AlCl_3$:urea molar ratios of 1.2, 1.3, and 1.5 and $AlCl_3$/EMImCl ionic liquid with $AlCl_3$:EMImCl molar ratios of 1.0, 1.3, and 1.5. Only one obvious peak is evident at about 347 cm^{-1} in the Raman spectrum at a molar ratio of 1.2, which is confirmed as $AlCl_4^-$ specie by the well-studied $AlCl_3$/EMImCl ionic liquid. However, as the molar ratio increased to 1.3 and 1.5, except for the peak at 347 cm^{-1}, one strong peak is found at approximately 310 cm^{-1} in the Raman spectrum, which is confirmed as $Al_2Cl_7^-$ specie by the well-studied $AlCl_3$/EMImCl ionic liquid. In addition, an increase in the intensity for the peak of $Al_2Cl_7^-$ specie and a decrease in the intensity for the peak of $AlCl_4^-$ specie are observed. The identical aluminum species and the similar variation of aluminum species with the molar ratio has also been found in the $AlCl_3$-based ionic liquids [30–34].

3.2. Cyclic voltammetry

To study the electrochemical behavior of aluminum and the effect of molar ratio of $AlCl_3$:urea on the reduction of Al(III) ions, CVs were carried out in $AlCl_3$/urea ionic liquid with $AlCl_3$:urea molar ratios of 1.2, 1.3, and 1.5 on a tungsten electrode at 333 K. Fig. 2 presents the cyclic voltammograms of $AlCl_3$/urea ionic liquid with $AlCl_3$:urea molar ratios of 1.2, 1.3, and 1.5. No obvious current is evident in the cyclic voltammogram at a molar ratio of 1.2, indicating that Al(III) is not reduced to aluminum metal at this molar ratio because of the formation of unreduced $AlCl_4^-$ specie as confirmed by Raman spectra analysis. However, as the molar ratio increased to 1.3, increase in cathodic and an anodic current is observed. A cathodic current with onset potential at about –0.20 V is observed during the cathodic scan, while an anodic wave with peak potential at about 0.10 V is observed during the anodic scan.

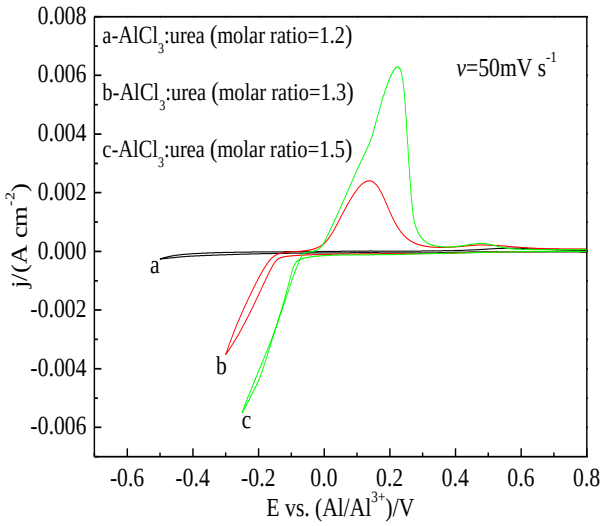

Figure 2. Cyclic voltammograms of $AlCl_3$/urea ionic liquid with $AlCl_3$:urea molar ratios of 1.2, 1.3, and 1.5 recorded on a tungsten electrode at 333 K. The scan rate was 50 mV s^{-1}.

To identify the cathodic and anodic reactions, a potentiostatic electrolysis experiment was conducted at −0.25 V, and the product obtained from electrolysis was characterized to be metallic aluminum using XRD analysis. Thus, it can be concluded that the reduction and oxidation currents correspond to bulk electrodeposition and stripping of aluminum. Further increase in the molar ratio to 1.5, shifted the onset potential of Al(III) toward more positive values, suggesting that Al(III) is more likely to be electrochemical reduced to aluminum metal at high molar ratio. This finding is best explained as an increase in the number of aluminum electroactive ($Al_2Cl_7^-$) species in the ionic liquid due to the increased molar ratio as confirmed by Raman spectra analysis. The similar electrochemical behavior of Al(III) has also been reported in literature [24,25,28–30].

3.3. Electrodeposition and characterization of aluminum

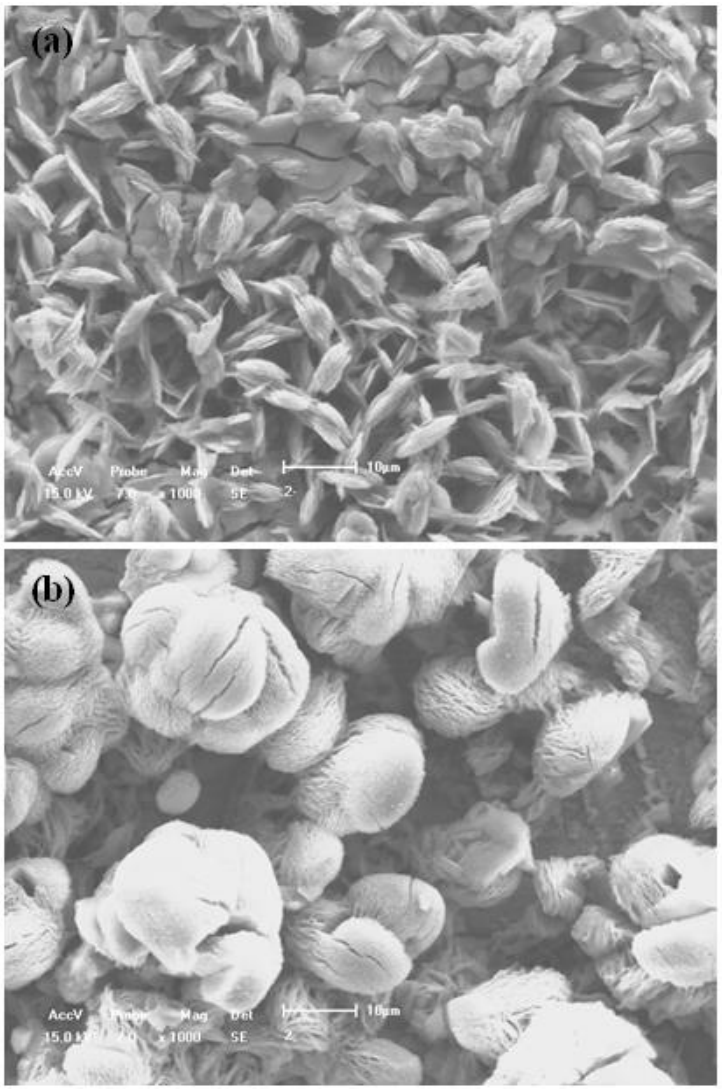

Figure 3. SEM micrographs of aluminum electrodeposits obtained from $AlCl_3$/urea ionic liquid with $AlCl_3$:urea molar ratios of 1.3 at −0.25 V for 2 h on a copper substrate at different temperatures: (a) 313 K, (b) 333 K.

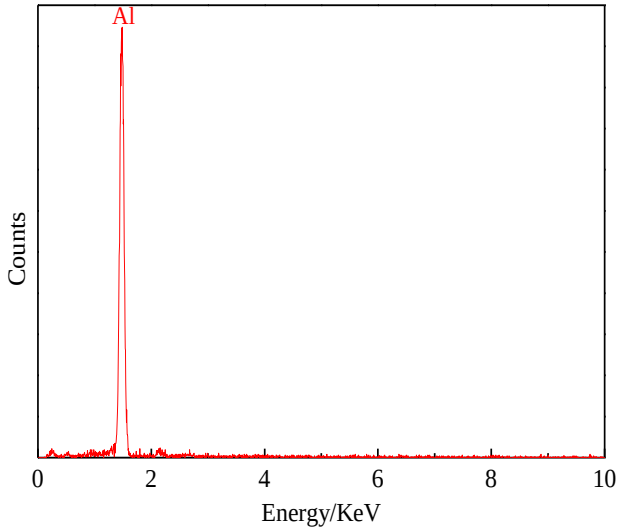

Figure 4. EDS spectrum of the aluminum electrodeposit obtained from $AlCl_3$/urea ionic liquid with $AlCl_3$:urea molar ratios of 1.3 on a copper substrate at −0.25 V and 333 K for 2 h.

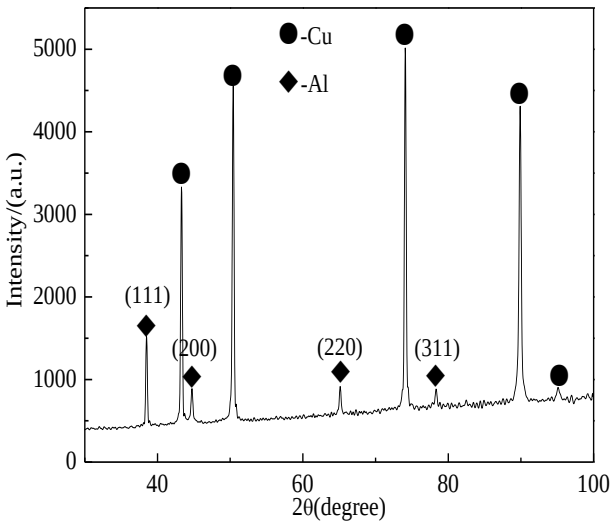

Figure 5. XRD pattern of the aluminum electrodeposit obtained from $AlCl_3$/urea ionic liquid with $AlCl_3$:urea molar ratios of 1.3 on a copper substrate at −0.25 V and 333 K for 2 h.

Fig. 3 shows the surface morphology of aluminum coatings obtained from $AlCl_3$/urea ionic liquid with $AlCl_3$:urea molar ratios of 1.3 at −0.25 V and at 313 K and 333 K for 2 h. Needle-like structures are obtained at 313K, while cauliflower-like structures are obtained at 333 K. These morphological differences reflect an increase in deposition rate with increasing temperature. The chemical composition of the obtained coating was also analyzed using EDS. The EDS spectrum of the coating only shows peak for aluminum, shown in Fig. 4, indicating that the chemical composition of the electrodeposit is metallic aluminum. No signals of other elements, such as O and Cl, are observed, indicating that the deposit is free of residual ionic liquid.

Fig. 5 presents the XRD pattern of the obtained coating from $AlCl_3$/urea ionic liquid with $AlCl_3$:urea molar ratios of 1.3 on a copper substrate at −0.25 V and 333 K for 2 h. It can been seen that

all the marked peaks are attributed to aluminum and the copper substrate, further indicating that the obtained coating is metallic aluminum. The obtained aluminum electrodeposit exhibits four clear diffraction peaks (111), (200), (220), and (311), and the diffraction peak (111) is the highest, indicating that there is a preferred orientation direction. No other obvious peaks are observed, indicating that the aluminum deposit with high-purity is obtained.

4. CONCLUSIONS

$AlCl_3$/urea ionic liquid was used to investigate the electrodeposition behavior of aluminum. Cathodic and anodic currents due to the bulk electrodeposition and stripping of aluminum were determined within the molar ratio range of 1.3 to 1.5, Al(III) is more likely to be electrochemical reduced in ionic liquids of higher molar ratios. Peaks due to $AlCl_4^-$ and $Al_2Cl_7^-$ species were determined in the Raman spectra. In addition, the intensity of peaks for $AlCl_4^-$ and $Al_2Cl_7^-$ species decreases and increases, respectively, with increasing the molar ratio of the ionic liquid. Potentiostatic electrolysis experiments were conducted at 313 K and at 333 K. Needle-like and cauliflower-like structures, both identified by EDS and XRD as metallic aluminum, were respectively electrodeposited at 313 K and at 333 K.

ACKNOWLEDGEMENTS
The authors would like to express their gratitude for the financial support provided by the National Natural Science Foundation of China (Grant Nos. 51904068, 51834004), the Natural Science Foundation of Liaoning Province of China (Grant No. 2019-BS-088), the China Postdoctoral Science Foundation (Grant No. 2018M630298) and Postdoctoral Science Foundation from Northeastern University of China (Grant No. 20180202), and the Fundamental Research Funds for the Central Universities (Grant No. N172503018).

References

1. J.W. Tang and K. Azumi, *Electrochim. Acta*, 56 (2011) 1130.
2. S.H. Yang and H. Knickle, *J. Power Sources*, 112 (2002) 162.
3. C.S. Li, W.Q. Ji, J. Chen and Z.L. Tao, *Chem. Mater.*, 19 (2007) 5812.
4. I. Smoljko, S. Gudic, N. Kuzmanic and M. Kliskic, *J. Appl. Electrochem.*, 42 (2012) 969.
5. M.-C. Lin, M. Gong, B.G. Lu, Y.P. Wu, D.-Y. Wang, M.Y. Guan, M. Angell, C.X. Chen, J. Yang, B.-J. Hwang and H.J. Dai, *Nature*, 520 (2015) 325.
6. Y.P. Wu, M. Gong, M.-C. Lin, C.Z. Yuan, M. Angell, L. Huang, D.-Y. Wang, X.D. Zhang, J. Yang, B.-J. Hwang and H.J. Dai, *Adv. Mater.*, 289 (2016) 218.
7. S. Wang, S.Q. Jiao, J.X. Wang, H.-S. Chen, D.H. Tian, H.P. Lei and D.-N. Fang, *ACS Nano*, 11 (2017) 469.
8. H. Chen, F. Guo, Y.J. Liu, T.Q. Huang, B.G. Zheng, N. Aanth, Z. Xu, W.W. Gao and C. Gao, *Adv. Mater.*, 29 (2017) 1605958.
9. D.-Y. Wang, C.-Y. Wei, M.-C. Lin, C.-J. Pan, H.-L. Chou, H.-A. Chen, M. Gong, Y.P. Wu, C.Z. Yuan, M. Angell. Y.-J. Hsieh, Y.-H. Chen, C.-Y. Wen, C.-W. Chen. B.-J. Hwang, C.-C. Chen and H.J. Dai, *Nat. Commun.*, 8 (2017) 1.
10. W. Kaveevivitchai, A. Hua, S.F. Wang, M.J. Park and A. Manthiram, *Small*, 13 (2017) 1701296.
11. A. Eftekhari and P. Corrochano, *Sustainable Energy Fuels*, 1 (2017) 1246.

12. K.V. Kravchyk, S.T. Wang, L. Piveteau and M.V. Kovalenko, *Chem. Mater.*, 29 (2017) 4484.
13. S. Wang, S.Q. Jiao, D.H. Tian, H.-S. Chen, H.D. Jiao, J.G. Tu, Y.J. Liu and D.-N. Fang, *Adv. Mater.*, 28 (2017) 1606349.
14. T. Jiang, M.J. Chollier Brym, G. Dube, A. Lasia and G.M. Brisard, *Surf. Coat. Technol.*, 201 (2006) 1.
15. B. Li, C.H. Fan, Y. Chen, J.W. Lou and L.G. Yan, *Electrochim. Acta*, 56 (2011) 5478.
16. A. Bakkar and V. Neubert, *Electrochim. Acta*, 103 (2013) 211.
17. A. Bakkar and V. Neubert, *Electrochem. Commun.*, 51 (2015) 113.
18. Q.X. Liu, S.Z.E. Abedin and F. Endres, *Surf. Coat. Technol.*, 201 (2006) 1352.
19. T. Tsuda, C.L. Hussey, G.R. Stafford and J.E. Bonevich, *J. Electrochem. Soc.*, 150 (2003) C234.
20. T. Tsuda, C.L. Hussey and G.R. Stafford, *J. Electrochem. Soc.*, 151 (2004) C379.
21. T. Tsuda, C.L. Hussey, G.R. Stafford and O. Kongstein, *J. Electrochem. Soc.*, 151 (2004) C447.
22. T. Tsuda, S. Arimoto, S. Kuwabata and C.L. Hussey, *J. Electrochem. Soc.*, 155 (2008) D256.
23. T. Tsuda and C.L. Hussey, *Thin Solid Films*, 516 (2008) 6220.
24. Y.X. Fang, X.G. Jiang, X.-G. Sun and S. Dai, *Chem. Commun.*, 51 (2015) 13286.
25. Y.X. Fang, K. Yoshii, X.G. Jiang, X.-G. Sun, T. Tsuda, N. Mehio and S. Dai, *Electrochim. Acta*, 160 (2015) 82.
26. S.Z.E. Abedin, E.M. Moustafa, R. Hempelmann, H. Natter and F. Endres, *ChemPhysChem*, 7 (2006) 1535.
27. P. Giridhar, S.Z.E. Abedin and F. Endres, *J. Solid State Electrochem.*, 16 (2012) 3487.
28. M. Li, B.L. Gao, C.Y. Liu, W.T. Chen, Z.N. Shi, X.W. Hu and Z.W. Wang, *Electrochim. Acta*, 180 (2015) 811.
29. M. Li, B.L. Gao, W.T. Chen, C.Y. Liu, Z.W. Wang, Z.N. Shi and X.W. Hu, *Electrochim. Acta*, 185 (2015) 148.
30. M. Li, B.L. Gao, C.Y. Liu, W.T. Chen, Z.W. Wang, Z.N. Shi and X.W. Hu, *J. Solid State Electrochem.*, 21 (2017) 469.
31. F. Coleman, G. Srinivasan, M.S. Kwasny, *Angew. Chem. Int. Ed.*, 52 (2013) 12582.
32. P.C. Hu, R. Zhang, X.H. Meng, H.Y. Liu, C.M. Xu, Z.C. Liu, *Inorg. Chem.*, 55 (2016) 2374.
33. C.Y. Liu, W.T. Chen, Z.M. W, B.L. Gao, X.W. Hu, Z.N. Shi, Z.W. Wang, *J. Mol. Liq.*, 247 (2017) 57.
34. P.C. Hu, W. Jiang, L.J. Zhong, S.F. Zhou, *RSC Adv.*, 8 (2018) 13248.